

Novel surface universality classes with strong anisotropy

B. Schmittmann¹, Gunnar Pruessner^{1,2}, and H.-K. Janssen³

Abstract. Using renormalized field theory, we examine the dynamics of a growing surface, driven by an obliquely incident particle beam. Its projection on the reference (substrate) plane selects a "parallel" direction, so that the evolution equation for the surface height becomes anisotropic. The phase diagram of the model is controlled by the properties of an effective anisotropic surface tension. Our renormalization group analysis suggests the existence of a line of continuous transitions and a line of (potentially) first-order transitions, which meet at a multicritical point. The full scaling behavior for the continuous line and the multicritical point is discussed in detail. Two novel universality classes for scale-invariant surface fluctuations are found.

¹Center for Stochastic Processes in Science and Engineering,

Department of Physics, Virginia Tech, Blacksburg, VA 24061-0435, USA ;

²Department of Physics (C.M.T.H.), Imperial College, London SW 7 2BW, UK ;

³Institut für Theoretische Physik III, Heinrich-Heine-Universität, 40225 Düsseldorf, Germany

E-mail: schmittm@vt.edu, gunnar.pruessner@physics.org,
janssen@thphy.uni-duesseldorf.de

Submitted to: J. Phys. A: Math. Gen.

1. Introduction

The capability to grow nanoscale layers of atoms or molecules on a substrate forms an important part of modern nanotechnology. Particles emitted from a source are deposited on the growing surface whose characteristics are determined by parameters such as growth temperature, surface diffusion, bulk relaxation, and particle attachment vs detachment rates. In addition to being clearly relevant for device applications, such surface growth problems also constitute an important class of generic nonequilibrium phenomena [1, 2] which cannot be described in terms of standard equilibrium ensemble theory.

A key goal of both theoretical and experimental investigations is the characterization and understanding of the resulting surface morphology, especially in terms of its statistical properties such as spatial and temporal height-height correlations. While local features may play an important role for device performance, large-scale, long-time characteristics offer better opportunities for theoretical understanding. They

are often universal, i.e., independent of microscopic details, depending only on global constraints such as symmetries and conservation laws. Here, we will explore the consequences of a reduced symmetry, which results if the particles arrive under an oblique (non-normal) angle.

Let us briefly review different classes of models for surface growth. The first issue is whether surface overhangs and shadowing effects can be neglected. For models with near-grazing incidence, this is usually a poor approximation. Focusing on vapor-deposited thin films, Meakin and Krug [3, 4, 5] considered ballistic deposition under these conditions. They found that columnar patterns form which shield parts of the growing surface from incoming particles and characterized these structures in terms of anisotropic scaling exponents, differentiating parallel and transverse directions [5, 6]. In contrast, for normal or near-normal incidence, overhangs and shadowing can often be neglected, and a description in terms of a stochastic equation of motion for a single-valued height variable becomes possible. A second important issue is whether particles, once attached to the surface, can desorb again. If desorption does occur, the surface relaxation is not conserved, and the leading nonlinearity in the Langevin equation is of the Kardar-Parisi-Zhang form [7]. Models of this type are most appropriate for chemical vapor deposition (see, e.g., [8, 9]) and sputtering processes [10]. Anisotropies have also been included by different authors [11, 12, 13]. In contrast, desorption can often be neglected in MBE-type processes which occur at low growth temperatures (see, e.g., [14]). In this case, the surface relaxation terms in the Langevin equation conserve the number of particles. For models of this type, the universal behavior depends on whether the incident beam is normal to the substrate or not. For normal incidence, the system remains isotropic on large scales while oblique incidence generates anisotropies which persist under coarse-graining. While the former case has been investigated extensively (see, e.g., [15, 16]), only partial results are available for the latter [17]. Noting that the reduced symmetry generates novel leading nonlinearities suggesting potentially distinct universal behavior, we consider surface growth under oblique incidence more systematically in the following.

Our analysis begins with a model first suggested by Marsili et al. [17] to describe MBE-type or ballistic deposition processes with oblique particle incidence. Based on a coarse-grained description in terms of a Langevin equation, the model adopts an idealized perspective [18, 19, 20], neglecting particle desorption and bulk defect formation. As a result, the surface relaxation becomes mass-conserving and can be written as the gradient of a current, in an appropriate reference frame. In contrast, the noise term in the Langevin equation is not mass-conserving, since it models the random arrivals of particles. Anisotropies emerge naturally in the Langevin equation, since the particle beam selects a preferred ("parallel") direction in the substrate plane. Extending the analysis of [17], we explore the consequences of an effective anisotropic surface tension. Generated by the interplay of interatomic interactions and kinetic effects, such as Schwoebel barriers, it plays a central role for the long-time, long-distance properties of the model. Due to the anisotropy, it will generically take different values,

denoted κ and γ , in the parallel and transverse directions. Depending on which of these parameters vanishes first, ripple-like surface instabilities are expected, aligned transverse to the soft direction. This leads to four different regimes with potentially scale-invariant behaviors. We analyze these four regimes, identify the scale-invariant ones, and discuss the associated anisotropic roughness exponents, using techniques from renormalized field theory. The original theory of [17] is recovered only if both couplings, κ and γ , vanish simultaneously.

The paper is organized as follows. We first present the underlying Langevin equation for a single-valued height field and briefly review the physical origin of its constituents. We also give a full discussion of its symmetries which are important for the subsequent analysis. We then turn to the renormalization group (RG) analysis. Identifying a set of effective coupling constants, and exploiting a Ward identity following from a (continuous) tilt invariance, we compute the naively divergent one-particle irreducible (1PI) vertex functions to one-loop order near the upper critical dimension. We analyze the four different cases separately: (o) both κ and γ are positive; (i) κ remains positive while γ vanishes; (ii) κ vanishes while γ remains positive; and finally, (iii) both κ and γ vanish simultaneously. A renormalization group equation allows us to derive the scaling properties of correlation and response functions for those cases which possess infrared (IR) stable fixed points. We identify a complete set of critical exponents, including four different roughness exponents for each case. Two of these characterize real-space scans along and transverse to the beam direction, and the remaining two are needed to describe scattering (i.e. momentum space) data with parallel or transverse momentum transfer.

2. The model

If surface overhangs and shadowing effects are neglected, the surface can be described by a single-valued height field, $h(\mathbf{r};t)$. Here, \mathbf{r} denotes a d -dimensional vector in a reference (substrate) plane, and t denotes time. h is measured along the z -axis which is normal to the substrate plane. The no-overhang assumption can be justified a posteriori provided the interface roughness exponents are less than unity [17]. The time evolution of the interface is described by a Langevin equation, combining deterministic terms, $G[h]$, and the effects of randomness, η , in the form

$$\partial_t h = G[h] + \eta \quad (1)$$

The conserved nature of the (deterministic) surface relaxation can be captured by writing $G[h] = -\nabla \cdot \mathbf{F}[h]$. Several different terms, arising from surface diffusion and the incident flux, contribute to $G[h]$ and are discussed in the following.

The incident particle current has a normal component J_z and a component parallel to the substrate plane, J_k . For particles of finite size r_0 , the effective flux must be measured at a distance r_0 normal to the surface [21]. Since we focus on the long time, large distance characteristics of the growing surface, the corresponding contributions to

$G[h]$ can be written as a gradient expansion, neglecting higher order terms:

$$G_{\text{ux}}[h] = J_z + J_k \nabla^2 h + \frac{1}{2} J_z \nabla^4 h - r_0 J_k (\nabla^2 h) \nabla^2 h \quad (2)$$

The first two terms of Eq. (2) can be removed by transforming into an appropriate co-moving frame, via $h(r;t) \rightarrow h(r + J_k t; t) - J_z t$. Next, we consider the effects of diffusion along the surface. This restriction generates a quartic term, of the form [22]

$$G_{\text{di}} = -r^4 h \quad (3)$$

Several comments are in order. First, we note the presence of the term $r_0 J_z \nabla^2 h (\nabla^2 h)$ in Eq. (2). Similar terms can arise from a step edge (Schwoebel) barrier [23, 24, 19], coming with a negative sign, or a surface tension with a positive sign. This allows for the possibility that the net contribution $r^2 h$ might vanish, playing the role of a critical parameter. Even if we follow [17] and set it to zero in the bare theory, it is actually generated under RG transformations and therefore intrinsically present. Second, the full rotational symmetry within the d -dimensional space of the substrate is broken by the nonlinear term in Eq. (2). As a consequence, any coarse-graining of the microscopic theory should give rise to different couplings in the parallel and transverse subspaces, and this is in fact borne out under the renormalization group. If the full anisotropy is incorporated into the theory, restricting rotational invariance to the $(d-1)$ -dimensional transverse subspace, the Langevin equation (1) takes the form

$$\begin{aligned} \partial_t h = & \kappa \nabla_k^2 h + \gamma \nabla_\perp^2 h - \kappa \nabla_k^4 h - \frac{1}{2} \nabla_\perp^2 \nabla_k^2 h - \frac{\gamma}{2} (\nabla_\perp^2)^2 h \\ & + \nabla_k h \cdot (\kappa \nabla_k^2 h + \gamma \nabla_\perp^2 h) + \end{aligned} \quad (4)$$

after some minor renamings. Here, ∇_k (∇_\perp) denotes derivatives (gradients) in the parallel (transverse) subspaces. It should be noted that the nonlinearity has also been split into two distinct terms, with couplings κ and γ . The Langevin noise $\xi(r;t)$ models the random particle aggregation at the surface, with zero average and second moment

$$\langle \xi(r;t) \xi(r';t') \rangle = 2^{-1} (\delta(r - r') \delta(t - t')) \quad (5)$$

In principle, one could also incorporate a noise term of the form $2(D_\kappa \nabla_k^2 + D_\gamma \nabla_\perp^2) \cdot (\nabla_k h - \nabla_\perp h) \delta(t - t')$ generated by (conserved) particle diffusion. In comparison to the aggregation noise, this contribution turns out to be irrelevant. However, one could imagine situations where diffusion is extremely fast, and aggregation occurs only very infrequently, so that Eq. (5) should be replaced by its diffusive counterpart. This "conserved" ideal MBE [25, 20] is not considered here, and will be left for future study.

Eq. (4) can be written in terms of surface currents j_k and j_\perp , according to

$$\partial_t h = \nabla_k j_k - \nabla_\perp j_\perp + \quad (6)$$

with

$$\begin{aligned} j_k = & \nabla_k (\kappa h - \kappa \nabla_k^2 h - \frac{1}{2} \nabla_\perp^2 h) - \frac{\kappa}{2} (\nabla_k h)^2 + \frac{\gamma}{2} (\nabla_\perp h)^2; \\ j_\perp = & \nabla_\perp (\gamma h - \gamma \nabla_\perp^2 h - \nabla_k^2 h) - \gamma (\nabla_\perp h) (\nabla_k h); \end{aligned}$$

Eq. (4), or its equivalent form, Eq. (6), is the starting point for the field-theoretic analysis. Its behavior is determined by the leading terms in the gradient expansion. We

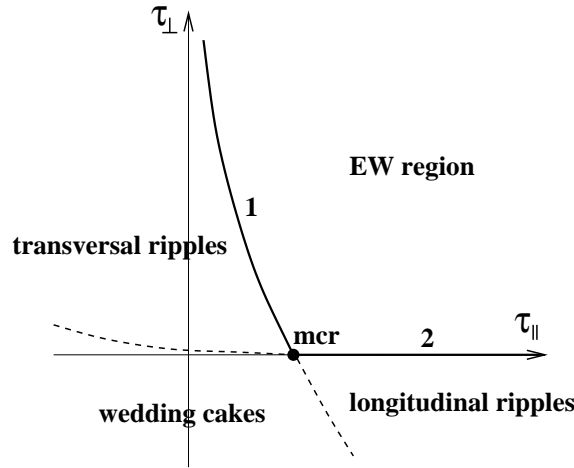


Figure 1. Sketch of the phase diagram in $(\kappa; \gamma)$ space. EW denotes the Edwards-Wilkinson region. The line labelled 1 marks a line of (possibly) discontinuous transitions, and line 2 corresponds to continuous transitions, both to inhomogeneous structures. The dashed lines denote very qualitative transition lines between different structures, and mcr labels the multicritical point.

can gain some qualitative insight by considering the linear terms first. To ensure stability of the homogeneous phase, the coupling constants κ and γ must be positive, and the cross-coupling may not exceed $(\kappa\gamma)^{1/2}$. The two couplings κ and γ play the role of critical parameters. If both are positive, the nonlinearities become irrelevant, and the problem reduces to the (Gaussian) Edwards-Wilkinson equation [26]. In contrast, if one or both of them vanish, the surface develops characteristic spatial structures. These take the form of ripples (reminiscent of corrugated roofing), if only one of the two couplings goes through zero; if both couplings become negative, the surface develops mounds or "wedding cakes" [2]. Focusing only on the onset of these instabilities, four different cases emerge which are discussed systematically in the following section: (o) the linear theory $\kappa > 0, \gamma > 0$; (i) a line of continuous transitions $\kappa > 0, \gamma \rightarrow 0$; (ii) a line of possibly first order transitions $\kappa \rightarrow 0, \gamma > 0$; and (iii) the multicritical (critical end-) point $\kappa \rightarrow 0, \gamma \rightarrow 0$. The qualitative phase diagram is shown in Fig. (1).

3. Renormalization group analysis

3.1. The dynamic functional

To unify the discussion, we first recast the Langevin equation (6) as a dynamic field theory. In this formulation, all statistical averages are expressed as path integrals, with weight $\exp(-J)$. In order to treat correlation and response functions in an analogous manner, it is convenient to introduce a response field $\tilde{h}(r;t)$, and formulate the dynamic response functional, following standard methods [27, 28, 29]:

$$J[\tilde{h};h] = \int d^d x dt \tilde{h}^{-1} \partial_t h + \partial_k \tilde{h} \partial_k h + r \tilde{h}^2 : \quad (7)$$

Before we turn to any computational details, we argue that the model is renormalizable. In other words, in each loop order we need to add only those primitive counterterms which can be absorbed in a renormalization of the fields and the coupling constants. As a first step in this procedure, we consider the symmetries exhibited by (7) since they place constraints on possible counterterms. The invariance against a shift of coordinates in the z -direction leads to the symmetry $h(r;t) \rightarrow h(r;t) + a$. Hence, the surface height h arises in the functional only in form of derivatives. Second, the functional is invariant under tilts of the surface by an infinitesimal "angle" b , i.e., $h(r;t) \rightarrow h(r;t) + b \cdot r$ provided the tilt is accompanied by an appropriate change of the parameters, namely, $k \rightarrow k - b_k k$ and $\gamma \rightarrow \gamma - b_\gamma \gamma$. Further, particle conservation on the surface lead to the invariance transformation $\tilde{h}(r;t) \rightarrow \tilde{h}(r;t) + c$, $h(r;t) \rightarrow h(r;t) + 2c \cdot t$. Therefore, we have a $(d+2)$ -dimensional (infinitesimal) symmetry group

$$h(r;t) \rightarrow h(r;t) + a + b \cdot r + 2c \cdot t; \quad \tilde{h}(r;t) \rightarrow \tilde{h}(r;t) + c;$$

which does not change the form of the dynamic functional or the functional integration measure, provided it is accompanied by an appropriate transformation of the parameters k and γ . In addition, we have a discrete symmetry, namely, inversion invariance in the $(x_k; z)$ subspace:

$$h(x_k; r_z; t) \rightarrow h(-x_k; r_z; t); \quad \tilde{h}(x_k; r_z; t) \rightarrow \tilde{h}(-x_k; r_z; t);$$

Finally, of course, we have isotropy in the transverse subspace. These symmetries can be considered as the fundamental defining elements of ideal MBE processes.

The renormalizability of our model can now be argued, following standard methods [30, 31]. In each loop order, the successive construction of the perturbation series produces only primitive ultraviolet (UV) divergences, provided that all counterterms constructed in lower orders are included to cancel non-primitive divergences which appear in subdiagrams. If the regularization procedure respects the symmetries of the model, then the remaining primitive divergences also preserve the symmetries. Thus, these divergences have the same form as the relevant terms of the initial model and their counterterms can be absorbed in a renormalization of the initial parameters. This presumes, of course, that all relevant interaction terms (i.e., composite fields with coupling constants of positive naive dimension) with the correct symmetries have been included in the initial dynamic functional, and all irrelevant couplings have been omitted. With regards to our model, a straightforward analysis of the relevant diagrams shows that we have indeed captured all relevant terms in the original Langevin equation (4). Hence, the model is renormalizable.

3.2. Elements of perturbation theory: the four different cases

In this section, we assemble the basic components of the perturbative analysis, leaving technical details to the Appendix. We first write the dynamic functional, $J[\tilde{h}; h]$ as the

sum of two parts. $J_0[\tilde{h};h]$ contains the Gaussian terms of the theory,

$$J_0[\tilde{h};h] = \int d^d x dt \tilde{h} \left(\partial_t^2 + \kappa \partial_k^4 + \gamma (r_\perp^2)^2 + 2 \partial_k^2 r_\perp^2 + \kappa \partial_k^2 + \gamma r_\perp^2 \right) h \tilde{h}^O \quad (8)$$

while $J_1[\tilde{h};h]$ takes the nonlinear interactions into account:

$$J_1[\tilde{h};h] = \int d^d x dt \tilde{h} (\partial_k h) (\kappa \partial_k^2 h + \gamma r_\perp^2 h) \quad (9)$$

Arbitrary correlation and response functions can now be computed as functional averages with statistical weight $J[\tilde{h};h]$:

$$\langle h \rangle = \int D[h] D[\tilde{h}] e^{J[\tilde{h};h]} :$$

Due to the anisotropy, it is possible to rescale parallel and transverse lengths independently. Considering a simple rescaling of parallel lengths $x_\parallel \rightarrow x'_\parallel$, via $x_k \rightarrow x'_k$, the functional remains invariant provided $h \rightarrow h$, $\tilde{h} \rightarrow \tilde{h}$ and $\kappa \rightarrow \kappa$, $\gamma \rightarrow \gamma$ while $\partial_k \rightarrow \partial_k$ and $\partial_t \rightarrow \partial_t$. Likewise, if only transverse lengths are rescaled, via $r_\perp \rightarrow r'_\perp$, the functional remains invariant provided $h \rightarrow h$, $\tilde{h} \rightarrow \tilde{h}$ and $\gamma \rightarrow \gamma$, $\partial_k \rightarrow \partial_k$, $\partial_t \rightarrow \partial_t$ while $\kappa \rightarrow \kappa$ and $\partial_k \rightarrow \partial_k$. In addition, there is an overall length scale l which accounts for the dimension of fields and coupling constants under the renormalization group. When we consider the three different cases below, these scale invariances will allow us to define appropriate effective expansion parameters, in order to eliminate redundant couplings [32].

Our goal is to compute the Green functions $G_{N,N'}(fr;tg) = \langle h[h]^N \tilde{h}[\tilde{h}]^{N'} \rangle^{\text{cum}}$, i.e., the cumulant averages of all possible products of fields $h(r;t)$, $\tilde{h}(r;t)$, or equivalently, the associated one-particle irreducible (1PI) vertex functions, $\Gamma_{N,N'}(fr;tg)$, with N' (N) h (\tilde{h} -) amputated legs, order by order in a diagrammatic perturbation expansion. The notation $fr;tg$ is short-hand for the full space- and time-dependence of these functions. As a first step in this process, we collect the elements of perturbation theory and introduce their graphic representation. Using $\langle \cdot \rangle$ to denote averages taken with the (Gaussian) weight J_0 , we will need the bare propagator, $G_0(q;t) = \langle h(q;t) \tilde{h}(q^0;0) \rangle_0$; as well as the bare correlator, $C_0(q;t) = \langle h(q;t) h(q^0;0) \rangle_0$; both in spatial Fourier space. In the following, we write $\langle \cdot \rangle_q \equiv \langle \cdot \rangle$ as short-hand for $\langle \cdot \rangle_{\frac{d^d q}{(2\pi)^d}}$. Defining

$$(q) = \kappa q_k^4 + \gamma (q_\perp^2)^2 + 2 q_k^2 q_\perp^2 + \kappa q_k^2 + \gamma q_\perp^2 \quad (10)$$

we find

$$\begin{aligned} G_0(q;t) &= (t) \exp(- (q) t); \\ C_0(q;t) &= (q)^{-1} G_0(q;jt); \end{aligned} \quad (11)$$

Here the Heaviside function $\Theta(t)$ is defined with $\Theta(0) = 0$. Diagrammatically, these two functions are represented as lines:

$$G_0(q; t) = \text{---} \xrightarrow{q} 0$$

$$C_0(q; t) = \text{---} \xleftarrow{q} 0$$

Turning to the interaction terms, it is convenient to rewrite them in a symmetrized form. In Fourier space, the expression for the three-point vertex reads

$$V(q_1; q_2; q_3) = i \sum_k q_{1k} q_{2k} q_{3k} + \frac{1}{2} (q_1^2 q_3^2 + q_2^2 q_3^2) q_{1k} q_{2k} \quad (12)$$

with $q_1 + q_2 + q_3 = 0$. Our sign convention is such that all momenta attached to a vertex are incoming. Diagrammatically, the whole vertex is represented as

$$V(q_1; q_2; q_3) = \begin{array}{c} \nearrow q_2^2 \\ \leftarrow q_1 \\ \searrow q_3^2 \end{array}$$

Returning to Eqs. (8) and (9), we now perform dimensional analysis. In the (infrared) limit of small momenta and frequencies, the Gaussian part of the dynamic functional is dominated by different terms, depending on the behavior of the control parameters κ and γ .

Case (o). If both κ and γ are finite and positive, the theory turns out to be purely Gaussian. Quartic derivatives can be neglected in the infrared limit; as a result, $\langle q \rangle$ simplifies to $\langle q \rangle \sim \kappa q_k^2 + \gamma q_\perp^2$. Since both parallel and transverse momenta appear only quadratically here, it is natural to choose a momentum scale such that $\kappa / \gamma \sim 1$, and $\kappa / \gamma \sim 0$. Time t scales as ℓ^2 , and the fields have dimensions $h(r; t) / \ell^{(d-2)/2}$ and $\tilde{h}(r; t) / \ell^{(d+2)/2}$. The nonlinear couplings scale as $\kappa / \gamma \sim \ell^{d-2}$ and are therefore irrelevant in any dimension $d > 0$. The resulting theory is a simple anisotropic generalization of the Edwards-Wilkinson equation [26],

$$\partial_t h = \kappa \partial_k^2 h + \gamma r_\perp^2 h + \dots \quad (13)$$

The anisotropies in the quadratic terms affect only nonuniversal amplitudes and can be removed by a simple rescaling, without losing any information of interest. As is well known, the two-point correlation function scales as

$$C(r; t) = \ell^{2-d} c(t/\ell^2) \quad (14)$$

from which one immediately reads off the (isotropic) roughness exponent $\alpha = (2-d)/2$ and the dynamic exponent $z = 2$. For a detailed discussion see [2]. Since this case is so familiar, we will not consider it any further.

Case (i). If κ remains finite and positive but γ is infinitesimal, the two leading terms in the dynamic functional are $\gamma \tilde{h}(r_\perp^2)^2 h$ and $\kappa \partial_k^2 h$. Hence, even in the Gaussian

theory, parallel and transverse momenta already scale differently, reflected in the choice $\tilde{q}_\parallel^2 \propto j$ and $q_k^2 \propto j^2$. If we introduce an anisotropic scaling exponent via $q_k^2 \propto j^{1+\alpha}$, we recognize that $\alpha = 1$ at the tree level. Continuing with the two leading terms, we note $k^2 \propto j^{-\alpha}$, and set $\alpha = 1$ via a transverse rescaling with an appropriate λ . Time scales as j^4 , and $k^2 \propto j^{-\alpha}$ and j^2 are both irrelevant. The only strongly relevant parameter of the theory is $\alpha \propto j^{-2}$. Introducing the effective dimension $D = d + 1$, one finds $h(r;t) \propto (t)^{-(D-4)/2}$ and $\tilde{h}(r;t) \propto (t)^{-(D+4)/2}$. For the nonlinear couplings, we obtain $\alpha \propto j^{-(4-D)/2}$ and $k^2 \propto j^{D-2}$. Since D is clearly positive, the coupling k^2 becomes irrelevant. The upper critical dimension d_c for the theory is determined by α , via $0 = 4 - D$ which leads to $d_c = 3$. The invariant dimensionless effective expansion parameter is $k^{3=4} \alpha = (3-d)^2$ as shown by the rescaling $\alpha \rightarrow \lambda^{3=2} \alpha$, $k \rightarrow \lambda^{-2} k$. The resulting propagators are controlled by $(q) = q_\parallel^2 + k^2 q_k^2 + (q_\parallel^2)^2$ where the $(q_\parallel^2)^2$ -term determines the UV behavior and α plays the role of the IR cutoff. At the tree level, this case corresponds to a critical line parameterized by k .

Case (ii). Here, α remains finite while k^2 vanishes. The Gaussian part of the functional is dominated by $\tilde{h} @_k^4 h$ and $\alpha \tilde{h} r_\parallel^2 h$. Again, parallel and transverse momenta scale differently, but their roles are now reversed: $q_k^2 \propto j$ and $\tilde{q}_\parallel^2 \propto j^{1+\alpha}$, with $\alpha = 1$ at the tree level. Both k^2 and α scale as j^0 , while α and j^2 are irrelevant. Defining the effective dimension as $D = 2(d-1) + 1$, one still has $h(r;t) \propto (t)^{-(D-4)/2}$ and $\tilde{h}(r;t) \propto (t)^{-(D+4)/2}$; we also recover $t \propto j^4$. Now, however, the strongly relevant perturbation is $k^2 \propto j^2$. The two nonlinearities switch roles so that $k^2 \propto j^{(6-D)/2}$ and $\alpha \propto j^{D-2}$. Clearly, α is irrelevant in all dimensions while k^2 becomes marginal at the upper critical dimension $d_c = 7=2$. The invariant dimensionless effective expansion parameter follows from the rescalings as $k^{7=8} \alpha^{(d-1)=4} = (7-2d)^2$. The momentum dependence of the propagators simplifies to $(q) = k^2 q_k^2 + \alpha q_\parallel^2 + k^2 q_k^4$. As in the previous case, at the tree level this situation corresponds to a critical line parameterized by α . However, we will see below that the order of the transition may well become first order once fluctuations are included.

Case (iii). Finally, we consider the multicritical point where both α and k^2 vanish. Both momenta scale identically, as $q_k^2 \propto \tilde{q}_\parallel^2 \propto j$, so that $\alpha = 0$ at the tree level. Again, we may set $\alpha = 1$. One obtains $t \propto j^4$, $k^2 \propto j^{-\alpha} \propto j^2$, and $h(r;t) \propto (t)^{-(D-4)/2}$, $\tilde{h}(r;t) \propto (t)^{-(D+4)/2}$, with $D = d$. The full propagators come into play. Both nonlinear couplings, k^2 and α , have the same upper critical dimension $d_c = 6$. The effective expansion parameters are $w = \frac{p}{k}$, $u_k = \frac{7=8}{k} = (6-d)^2$, and $u_\alpha = \frac{3=8}{k} \alpha = (6-d)^2$. In this case, the anisotropy exponent vanishes at the tree level.

In the following, we analyze the three nontrivial cases in a one-loop approximation, using dimensional regularization combined with minimal subtraction [30, 31]. The essential components are the 1PI vertex functions $\Gamma_{N,N}(f;g)$. Focusing on the ultraviolet singularities, only those $\Gamma_{N,N}$ with positive engineering dimension are to be considered. Taking into account the symmetries and the momentum-dependence carried by the derivatives on the external legs, the set of naively divergent vertex functions is

reduced to $\chi_{1,1}$ and $\chi_{1,2}$. Specifically, at the upper critical dimension of cases (ii) and (iii), $\chi_{1,1}$ is quadratically divergent and $\chi_{1,2}$ is marginal. In case (i), $\chi_{1,1}$ is already marginal after accounting for the external momenta.

3.3. Perturbation theory.

In this section, we summarize the calculation of $\chi_{1,1}$ and $\chi_{1,2}$, to one loop order. Details are relegated to the Appendix.

The main features which recur in all three cases are the following. If $\chi_{1,1}$ is quadratically divergent, this divergence is first removed by an additive renormalization, i.e., a shift of the critical parameter(s). Specifically, the true critical point is located through the singularity of the parallel and/or transverse static susceptibilities, χ_k and χ_q , defined by

$$\begin{aligned} \chi_k^{-1} &= \lim_{q_k \rightarrow 0} q_k^{-2} \chi_{1,1}(q_k; q_\perp = 0; \omega = 0) \\ \chi_q^{-1} &= \lim_{q_\perp \rightarrow 0} (q_\perp^2)^{-1} \chi_{1,1}(q_k = 0; q_\perp; \omega = 0) \end{aligned} \quad (15)$$

We find that nontrivial shifts are only required for cases (ii) and (iii), and only for χ_k .

The remaining logarithmic divergences are then computed using dimensional regularization, so that ultraviolet divergences appear as simple poles in $\epsilon = d_c - d$. In a minimal subtraction scheme, we focus exclusively on these poles and their amplitudes. Since the nonlinearities are cubic in the field, the expansion is organized in powers of u_k^2 , u_\perp^2 , and $u_k u_\perp$; i.e., the first correction to the tree level is always quadratic for $\chi_{1,1}$ and cubic for $\chi_{1,2}$. The tilt invariance leads to a Ward identity connecting $\chi_{1,1}$ and $\chi_{1,2}$, namely,

$$\begin{aligned} i \frac{\partial}{\partial q_k^0} \chi_{1,2}(q; \omega; q_\perp^0; \omega_\perp^0) &= -k \frac{\partial \chi_{1,1}(q; \omega)}{\partial q_k} + \perp \frac{\partial \chi_{1,1}(q; \omega)}{\partial q_\perp} \\ i \frac{\partial}{\partial q_\perp^0} \chi_{1,2}(q; \omega; q_\perp^0; \omega_\perp^0) &= 0 \end{aligned} \quad (16)$$

Here, $(q; \omega)$ and $(q^0; \omega^0)$ denote the momenta and frequencies labelled with subscripts 2 and 3 in Eq. (12). By virtue of this symmetry, it will be sufficient to compute $\chi_{1,1}$ in order to extract the renormalization of all parameters, including those of the coupling constants χ_k and χ_\perp . More specifically, the tilt transformation $h(r; t) \rightarrow h(r; t) + b \cdot r$, $k \rightarrow k - b_k$, $\perp \rightarrow \perp - b_\perp$ shows that the parameter b renormalizes as the field h itself. Hence, the term $\chi_k h$ renormalizes exactly like χ_k , and $\chi_\perp h$ like χ_\perp .

Next, we collect a few general properties of the diagrams contributing to $\chi_{1,1}(q; \omega)$ which follow from the special form of the interactions, Eq. (9). We first consider diagrams where the external h -leg carries two transverse derivatives. Such diagrams can arise only from the interaction $\perp \nabla_k h \nabla_\perp^2 h$. Thanks to particle conservation, all these graphs sum in such a way as to generate at least one spatial derivative on the external ∇ -leg. Moreover, either parallel inversion or transverse rotation symmetry guarantees that, in fact, there are at least two such derivatives. Thus, there are no

corrections to the term $\frac{1}{2} \tilde{h} r^2 \tilde{h}$ in J_0 , Eq. (8). Similarly, since external \tilde{h} - and h -legs always come with at least one spatial derivative, there are no perturbative contributions to the terms $\tilde{h} \partial_t h$ and \tilde{h}^2 . Hence, these three terms are not renormalized. Further, if the coupling constant γ is zero, as in case (ii), only diagrams with parallel derivatives on all legs are generated, and so operators carrying no parallel, or mixed parallel and transverse, derivatives suffer no renormalization. In contrast, when $\gamma \neq 0$, there is no such simplification since this vertex can contribute to purely "parallel" terms. If both coupling constants κ and γ are nonzero, they mix under the RG, and we have to renormalize the couplings by matrices, rather than simple multiplicative factors.

With these considerations in mind, we propose the following renormalization scheme:

$$\begin{aligned}
 h &\rightarrow h = Z^{1/2} h & \tilde{h} &\rightarrow \tilde{h} = Z^{-1/2} \tilde{h} & \gamma &\rightarrow \gamma \\
 \gamma &\rightarrow \gamma = Z^{-1} \gamma & \kappa &\rightarrow \kappa = Z^{-1} (Z \kappa + \frac{1}{2} Y \gamma) + \kappa_{\text{pc}} \\
 \kappa &\rightarrow \kappa = Z^{-1} \kappa & \kappa &\rightarrow \kappa = Z^{-1} \kappa
 \end{aligned} \quad (17)$$

κ_{pc} accounts for the shift of the critical point in cases (ii) and (iii). The Ward identities then lead to the renormalizations

$$\gamma \rightarrow \gamma = Z^{3/2} \gamma \quad \kappa \rightarrow \kappa = Z^{3/2} (Z \kappa + Y \gamma) : \quad (18)$$

The renormalization factors Z , Z , Z , Z , and Y must be calculated from the "poles of the dimensionally regularized perturbation series of $\Gamma_{1,1}(q; \epsilon)$: In minimal subtraction, they are of the form $Z = 1 + \sum_{n=1}^{\infty} Z^{(n)} \epsilon^n$, $Y = \sum_{n=1}^{\infty} Y^{(n)} \epsilon^n$, where the $Z^{(n)}$ and $Y^{(n)}$ are expansions in the renormalized effective coupling constants. Here, the subscript stands as a placeholder for any member of the set of indices. The individual characteristics of the three cases of interest are now treated sequentially.

Case (i): $\gamma \neq 0$ and $\kappa \neq 0$. This is the simplest non-trivial case. Only one parameter, γ , needs to be tuned to access criticality. Since κ is irrelevant, it may be set to zero. Neglecting all other irrelevant terms as well, the functional simplifies to

$$J = \int d^d x dt \tilde{h} [-\partial_t + (r^2/2) - \kappa \partial_k^2 - \gamma r^2] h - \tilde{h}^2 - \gamma \tilde{h} (\partial_k h) r^2 h \quad (19)$$

In this case $\kappa = \gamma = \kappa = Y = 0$. All divergences are parameterized by $\epsilon = d_c - d$ where $d_c = 3$.

Following standard methods (for details see Appendix A), we obtain the following expression for the singular part of the two-point vertex function,

$$\Gamma_{1,1}(q; \epsilon) = i! + [\kappa q_k^2 + (q^2/2)^2 + \gamma q^2] + \frac{u^2}{8\epsilon} [2 \kappa q_k^2 - (q^2/2)^2] + O(u^4) \quad (20)$$

where

$$u = A \epsilon^{3/4} \gamma^{-1/2} \epsilon^{-2} \quad (21)$$

is the effective expansion parameter. A is a geometric factor which appears in all integrals:

$$A = \frac{S_{d-1}}{(2\pi)^d} \Gamma\left(\frac{d}{2}\right) - \frac{1}{2} \epsilon^2 = \frac{1 + \epsilon^2}{2}$$

and S_d is the surface area of the d -dimensional unit sphere.

The renormalized vertex function $\Gamma_{1,1}$ is defined by demanding that

$$\Gamma_{1,1}(q; !; i; ?; i; k; u; i;) = \Gamma_{1,1}(q; !; i; i; ?; i; k; i; ?)$$

be pole-free. One finds

$$Z = 1 + \frac{u^2}{8''} + O(u^4); \quad Z = 1 - \frac{u^2}{4''} + O(u^4); \quad (22)$$

The corresponding Wilson functions are defined as the logarithmic derivatives of the associated Z -factors, at constant bare quantities, i.e., $\partial \ln Z / \partial \bar{g}_{\text{bare}}$. The logarithmic derivatives of the control parameters and of the relaxation coefficient are then given by

$$\begin{aligned} \partial \ln \bar{g}_{\text{bare}} &= \quad ; \\ \partial \ln \bar{?}_{\text{bare}} &= \quad ; \\ \partial \ln \bar{g}_{\text{bare}} &= \quad ; \end{aligned} \quad (23)$$

The flow of the dimensionless effective coupling constant u under renormalization is controlled by the Gell-Mann-Low function,

$$\partial u / \partial \bar{g}_{\text{bare}} = u \left[-\frac{''}{2} + \frac{3}{4} (+) \right]; \quad (24)$$

The renormalizability of the theory demands that all the Wilson functions be free of $''$ -poles; moreover, in minimal subtraction it can be shown [30] that the perturbative corrections do not contain $''$ any more. It is easy to demonstrate that all Wilson functions are determined by the first term, $Z^{(1)}$, in the Laurent expansion of the Z -factors. So, we obtain

$$\begin{aligned} (u) &= \frac{u}{2} \frac{\partial Z^{(1)}}{\partial u} = -\frac{u^2}{8} + O(u^4); \\ (u) &= \frac{u}{2} \frac{\partial Z^{(1)}}{\partial u} = \frac{u^2}{4} + O(u^4); \\ (u) &= u \left[-\frac{''}{2} + \frac{3}{32} u^2 + O(u^4) \right]; \end{aligned} \quad (25)$$

The renormalization group equation (RGE) for the Green functions simply states that the bare theory is independent of the external momentum scale :

$$\begin{aligned} 0 &= \frac{d}{d} G_{N, N'}(fr; tg; ?; i; k; i; ; ?) \\ &= \frac{d}{d} Z^{(N - N')=2} G_{N, N'}(fr; !g; ?; i; k; u; i; ;) : \end{aligned} \quad (26)$$

Explicitly, this partial differential equation becomes

$$h \frac{\partial}{\partial} + \frac{\partial}{\partial u} - \frac{\partial}{\partial} + ? \frac{\partial}{\partial ?} + (\quad) k \frac{\partial}{\partial k} + \frac{1}{2} (N - N') G_{N, N'} = 0; \quad (27)$$

It will lead to asymptotic scaling, provided (u) possesses an infrared stable fixed point u^* , i.e., a solution of $(u) = 0$ with $\partial(u) / \partial u > 0$. To one loop order, Eq. (25) allows for a single fixed point with the desired properties, namely,

$$u^* = -4 \frac{''}{3} (1 + O('')) ; \quad (28)$$

where the sign is determined by the sign of the initial coupling constant g_0 . Clearly, this u is non-zero in the ϵ -expansion. Under the (reasonable) assumption that the full (resummed) series for $u(\epsilon)$ is non-zero at the integer values of ϵ corresponding to physical dimensions, Eq. (24) gives us the exact relation

$$u(4) + u(6) = \frac{2}{3} \quad (29)$$

In the following, Wilson β -functions, evaluated at the fixed point, will simply be denoted by a superscript $*$.

The solution of the RGE (27) is easily found by applying the method of characteristics. At the stable fixed point u^* we obtain the scaling solution

$$G_{N,N'}(f; t; g; \epsilon; k; \epsilon; \epsilon) = l^{(N+N')=2} G_{N,N'}(f; t; g; l^{-\epsilon}; l^{-\epsilon} k; l^{-\epsilon}; l^{-\epsilon})$$

where l is an arbitrary flow parameter. The parallel and transverse scale invariances, together with dimensional analysis, give us an additional scaling relation for the Green functions, namely

$$G_{N,N'}(f; t; g; \epsilon; k; u; \epsilon; \epsilon) = l^{(N+N')=2 - N(D-4)=2 + N'(D+4)=2} G_{N,N'}(f l^{-2} x_k; l r; l^4 t; g l^{-2}; l^{-2} k; u; l; l)$$

Combining these two relations, choosing $l = l^{\epsilon=2}$ and recalling $D = d + 1$, we arrive at the final scaling form for the Green functions. Suppressing unneeded arguments, we can choose to write them in the form

$$G_{N,N'}(f; t; g; \epsilon) = l^{N,N'} G_{N,N'}(f l^{1+} x_k; l r; l^2 t; g l^{1-} \epsilon) \quad (30)$$

where the scaling exponents α and β can be expressed in terms of Wilson functions, evaluated at the fixed point:

$$\alpha = 1 + \frac{\gamma_g}{2}; \quad \beta = \frac{\gamma_g}{2} \quad (31)$$

Since we have only two independent renormalizations, the remaining exponents follow from scaling laws, namely,

$$z = 4 - \alpha; \quad 1 - \beta = 2 - \alpha; \quad (32)$$

and

$$N_{N,N'} = \frac{N}{2} (d + 4 + \alpha) + \frac{N'}{2} (d + 4 + \beta) \quad (33)$$

Eq. (29), provided it holds, can be exploited to give another exponent identity:

$$\alpha + \beta = 2 - d = 3: \quad (34)$$

To conclude, only a single exponent, e.g., α has to be computed order by order in perturbation theory. Then, all others follow from exponent identities which are exact, at least within perturbation theory. Our one-loop calculation results in

$$\alpha = 2\epsilon = 3 + O(\epsilon^2): \quad (35)$$

Case (ii): $\kappa \neq 0$ and $\gamma \neq 0$. This is the second non-trivial case. Neglecting irrelevant terms, the dynamic response functional simplifies to

$$J[\mathbf{h}; h] = \int d^d x dt \left[\frac{1}{2} \dot{\mathbf{h}}^2 + \frac{1}{2} \kappa \mathbf{h}^4 + \frac{1}{2} \kappa \mathbf{h}^2 + \frac{1}{2} \gamma \mathbf{h}^2 \right] + \int d^d x dt \left[\frac{1}{2} \dot{\mathbf{h}}^2 + \frac{1}{2} \kappa \mathbf{h}^4 + \frac{1}{2} \kappa \mathbf{h}^2 + \frac{1}{2} \gamma \mathbf{h}^2 \right] \quad (36)$$

In this case, we define $\epsilon = d_c - d$ with $d_c = 7/2$.

Since $\chi_{1,1}(q; !)$ is quadratically divergent in this case, an additive renormalization of the critical parameter, κ , is required (see Appendix B). Once this is accounted for, we obtain the following one-loop expression for the singular part of $\chi_{1,1}$:

$$\chi_{1,1}(q; !)_{\text{pole}} = i! + \frac{1}{2} \kappa q_k^4 + \frac{1}{2} \kappa q_k^2 + \frac{1}{2} \gamma q_\gamma^2 + \frac{u^2}{2} \left[\kappa q_k^4 + \kappa q_k^2 + \dots \right] \quad (37)$$

where u is the effective expansion parameter now defined as

$$u = B \frac{7-8}{\kappa} \frac{(d-1)=4}{\gamma} \frac{(7-2d)=2}{\kappa} \quad (38)$$

with a geometric factor

$$B = \frac{S_{d-1}}{2(2-\epsilon)^d} = \frac{d-1}{2} \frac{d}{2} (1 + \epsilon) :$$

Eq. (37) gives rise to renormalizations of κ and γ . Since the vertex κ carries only parallel momenta in this case, there are no contributions of order q_γ^2 at any order, implying the absence of field renormalizations. Hence, $Z = 1$. The remaining poles are absorbed into the renormalization factors

$$\begin{aligned} Z_\kappa &= 1 - \frac{u^2}{2} + O(u^4); \\ Z_\gamma &= 1 - \frac{u^2}{2} + O(u^4); \end{aligned} \quad (39)$$

Defining the Gell-Mann-Low function of u , as well as the Wilson functions, in analogy to the previous case, we obtain

$$\begin{aligned} \beta(u) &= \epsilon \ln Z_\kappa \bar{\kappa}_{\text{bare}} = u^2 + O(u^4); \\ \gamma(u) &= \epsilon \ln Z_\gamma \bar{\gamma}_{\text{bare}} = u^2 + O(u^4); \\ \beta_1(u) &= u \left[-\epsilon + \frac{7}{8} \right] = u \left[-\epsilon + \frac{1}{8} u^2 + O(u^4) \right] \end{aligned} \quad (40)$$

The fixed point equation $\beta(u) = 0$ does not yield a stable real fixed point, at least to this order in perturbation theory. It remains an open question whether such a fixed point, and the associated scaling properties, might emerge at higher orders. Restricting ourselves to our current results, the absence of an infrared stable fixed point might suggest a first order transition. A more detailed analysis of the underlying mean-field theory or a careful computational study would be required to shed more light on this issue. Both are beyond the scope of this article.

Case (iii): $\kappa \neq 0$ and $\gamma \neq 0$. Finally, we turn to the analysis of the multicritical point. This situation was previously considered in [17], using a momentum shell decimation scheme. This procedure requires considerable care for field theories with

strong anisotropy and nonlinearities carrying multiple derivatives, since the corrections depend on the way in which the hard momentum cut-off is implemented. Moreover, the hard momentum shell cut-off introduces long-ranged correlations on the scale of the cut-off momentum which must be handled very carefully. Whatever the source of the discrepancies, even after meticulous checks we were unable to reproduce the earlier results.

The full functional, Eqs. (8) and (9), as well as the full (bare) propagators and correlators, Eq. (11), now come into play. To ensure the stability of the critical theory at the tree level, we demand $q_k^4 + 2 q_k^2 q_\perp^2 + (q_\perp^2)^2 = 0$. This limits the physical range of k and \perp to $k > 0$ and $\perp > \frac{p}{k}$. To complicate matters further, both nonlinear couplings, u_k and u_\perp , are marginal at the upper critical dimension $d_c = 6$. However we know that, thanks to the Ward identity, all renormalizations can still be obtained from the two-point function, $\Gamma_{1,1}$.

A first analysis of diagrams contributing to $\Gamma_{1,1}(q; !)$ shows that two of them are quadratically divergent. Since both of them carry a momentum prefactor of q_k^2 , they can be absorbed in an additive renormalization, i.e., a shift of the bare control parameter k , as remarked before. No shift of the bare \perp is needed.

Leaving details to Appendix C, our one-loop result for $\Gamma_{1,1}$ is now considerably more complex, thanks to the presence of both vertices. In order to eliminate redundant parameters, it is again convenient to define invariant dimensionless coupling constants, guided by the parallel and transverse rescalings:

$$\begin{aligned} u_k &= C'' \frac{7=8}{k} (1 + w)^{5=4} k^{(6-d)=2} ; \quad w = \frac{1=2}{k} ; \\ u_\perp &= C'' \frac{3=8}{k} (1 + w)^{5=4} \perp^{(6-d)=2} ; \end{aligned} \quad (41)$$

where the constant C'' is defined by

$$C'' = \frac{S_{d-1}}{(2\pi)^d} \frac{(1 + \epsilon=2)}{32 \pi^{\frac{d}{2}}}$$

The definition of the effective coupling constants contains a suitable w -dependent denominator, which is common to all integrals. Collecting the results from Appendix C, we find the singular parts

$$\begin{aligned} \Gamma_{1,1}(q; !)_{\text{pole}} &= i! + \frac{h}{q_k^2 (q_k^2 + k) + q_\perp^2 (q_\perp^2 + \perp) + 2 q_k^2 q_\perp^2} \frac{i}{k} \\ &+ \frac{1=2}{k} q_k^2 u_k^2 \frac{B_1}{w} \frac{1=2}{k} k + \frac{B_1}{w} \perp + u_\perp^2 \frac{B_2}{w} \frac{1=2}{k} k + \frac{B_3}{w} \perp \frac{i}{k} \\ &+ \frac{h}{k} q_k^4 u_k^2 \frac{C_1}{w} + u_\perp^2 \frac{C_2}{w} \frac{i}{k} (q_\perp^2)^2 u_\perp^2 \frac{A_1}{w} \\ &+ \frac{1=2}{k} q_k^2 q_\perp^2 u_k^2 \frac{D_1}{w} + u_\perp^2 \frac{D_2}{w} + u_k u_\perp \frac{D_3}{w} : \end{aligned} \quad (42)$$

Here, A_1, B_1, \dots, D_3 are w -dependent functions whose explicit forms are listed in Appendix C.

According to the general renormalization scheme, Eq. (17), the full set of renormalization factors now comes into play. At one loop order, we read off

$$\begin{aligned}
 Z &= 1 + A_1 \frac{u_?^2}{n} + O(u^4); \\
 Z &= 1 + B_1 \frac{u_k^2}{n} + B_2 \frac{u_?^2}{n} + O(u^4); \\
 Y &= B_1 \frac{u_k^2}{n} + B_3 \frac{u_?^2}{n} + O(u^4); \\
 Z &= 1 + C_1 \frac{u_k^2}{n} + C_2 \frac{u_?^2}{n} + O(u^4); \\
 Z &= 1 + D_1 \frac{u_k^2}{2w n} + D_2 \frac{u_?^2}{2w n} + D_3 \frac{u_k u_?}{2w n} + O(u^4);
 \end{aligned} \tag{43}$$

Here, $O(u^4)$ is short-hand for the two-loop corrections which are of fourth order in the couplings u_k and $u_?$. Denoting $\beta_{bare} = \frac{1}{2}(u_k \beta_{u_k} + u_? \beta_{u_?})Z^{(1)}$, $\gamma = \frac{1}{2}(u_k \beta_{u_k} + u_? \beta_{u_?})Y^{(1)}$ as before, one obtains to one loop order

$$\begin{aligned}
 &= 2(1+w)u_?^2; \quad \beta_{u_k} = 3u_k^2(5+2w)u_?^2; \\
 \gamma &= 3u_k^2 - 3(7+10w+4w^2)u_?^2; \\
 &= (3+w)u_k^2 - (5+9w+10w^2+4w^3)u_?^2; \\
 &= \frac{(7+5w)}{10w}u_k^2 - \frac{(49+65w+26w^2)}{10w}u_?^2 - \frac{(10+2w)}{10w}u_k u_?;
 \end{aligned} \tag{44}$$

We now consider the Gel'fand-Mann-Low functions for the three dimensionless effective couplings u_k , $u_?$, and w :

$$\begin{aligned}
 \beta_{u_k} &= \frac{n}{2} + \frac{5}{8} + \frac{7}{8} \frac{5-w}{4(1+w)} u_k - \gamma u_? \\
 \beta_{u_?} &= \frac{n}{2} + \frac{9}{8} + \frac{3}{8} \frac{5-w}{4(1+w)} u_? \\
 \beta_w &= \frac{1}{2} + \frac{1}{2} w
 \end{aligned} \tag{45}$$

We seek a set of fixed points $(w; u_k; u_?)$ such that all three β -functions vanish simultaneously. The eigenvalues of the linearized system, evaluated in the vicinity of each fixed point, provide information about its stability. If all of them are positive, the fixed point is infrared stable; otherwise, it is unstable in one or more directions.

There is only one nontrivial, physical (i.e., real) infrared stable fixed point given by

$$w = 2 \frac{n-3}{5} \left(1 + O(n^{-1}) \right); u_k = \frac{7^{n-3} \sqrt{15+25}}{11} n^{1=2} + O(n^{3=2}); u_? = 0 \tag{46}$$

For $u_? = 0$, we find another root $w = 1 - \frac{2}{5} \sqrt{15} < 1$, but this solution must be excluded since it leads to a linearly unstable theory (see the discussion after Eq. (6)). There are numerous fixed points with $u_? \neq 0$ and $u_k \neq 0$, but these are all infrared unstable or nonphysical, in the sense that either u_k or $u_?$ are imaginary or $w < 1$. In contrast to earlier results by [17], we do not find a physically viable fixed point with

$u_? \notin 0$. We have also carefully considered the possibility of "degenerate fixed points" with $w = 0$ or $w = 1$; none of these are stable.

Returning briefly to Eq. (42), we note that the critical parameter γ_k appears only in the combination $\gamma_k^{1=2} \gamma_k^{1=2}$, which is actually the appropriate scale-invariant form. This suggests a slight modification of the general renormalization scheme, Eq. (17), so that the renormalizations of the critical control parameters are now written as

$$\gamma_k = Z^{1=2} Z^{1=2} (\gamma_k + Y_?); \quad ? = Z^{1=2} ?; \quad (47)$$

Their derivatives can be expressed in terms of the β -functions of Eq. (44):

$$\begin{aligned} \frac{\partial \gamma_k}{\partial \gamma_k} &= \frac{1}{2} + \frac{1}{2} \gamma_k Y_?; \\ \frac{\partial ?}{\partial ?} &= ?; \end{aligned} \quad (48)$$

One can see quite easily that $u_? = 0$ is an invariant subspace of the RG, since the coupling u_k alone cannot generate any corrections to $u_?$. Assuming that the stable fixed point, at higher orders of perturbation theory, remains characterized by $w \notin 0, u_k \notin 0$, while $u_? = 0$, we can establish the (exact) relations

$$= 0; \quad \frac{7}{4} \quad 2 = "; \quad = \frac{1}{2} \quad (49)$$

which will lead to exponent identities, as we shall presently see. At the fixed point, the RGE takes the simplified form

$$h \frac{\partial}{\partial} \left(\frac{\partial}{\partial \gamma_k} + \left(\frac{1}{2} \right) \gamma_k Y_? \right) \frac{\partial}{\partial \gamma_k} G_{N,N} = 0; \quad (50)$$

The two critical control parameters $(\gamma_k; ?)$ are diagonalized by introducing the new independent variables $(\gamma_k; ?)$, defined by

$$\gamma_k = \gamma_k + \frac{2 Y_?}{2} ?; \quad (51)$$

This new critical control parameter γ_k takes over the role of γ_k in the mean-field approximation. The solution of the RGE (50) is given by

$$\begin{aligned} G_{N,N}(fr;tg;\gamma_k;?;\gamma_k;w;u_k;u_?;?) = \\ = F_{N,N}(fr;tg;l^{=2} \gamma_k;?;l \gamma_k;l); \end{aligned} \quad (52)$$

where l is an arbitrary scale, and $F_{N,N}$ results from $G_{N,N}$ after the variable transformation to $(\gamma_k; ?)$. Combining this equation with the simple parallel and transverse scale invariances, we arrive at the scaling form

$$G_{N,N}(fr;tg;\gamma_k;?) = l^{N,N} F_{N,N}(fl^{1+} x_k;lr;?;l^{1= \gamma_k} \gamma_k;l^{1= ?} ?); \quad (53)$$

where N,N is again given by Eq. (33) while the other exponents take the values

$$\begin{aligned} &= \frac{1}{4}; \quad = = 0; \quad z = 4 \quad = 4; \\ 1= \gamma_k &= 2 \quad \frac{1}{2} + ; \quad 1= ? = 2; \end{aligned} \quad (54)$$

The result to all orders, Eq. (49), leads to an exact relation between ν_k and ν :

$$\nu_k = \frac{2}{d-2+3\nu} : \quad (55)$$

Once again, only a single exponent must be computed explicitly within the ϵ -expansion, e.g., ν . Our one-loop calculation yields

$$\nu = \frac{23 + \frac{6}{d-15}}{11} \epsilon + O(\epsilon^2) ; \quad (56)$$

and for the mixing of the critical control parameters

$$\nu_k = \frac{\nu_k}{\nu_k} + \frac{17}{3(10 + \frac{6}{d-15})} \epsilon + O(\epsilon^2) : \quad (57)$$

Let us briefly return to the assumption that the stable fixed point is characterized by $u_2 = 0$. Thanks to Eq. (45) and the associated linear stability matrix, we can determine the stability criterion, i.e., the correction-to-scaling exponent of u_2 , to all orders in perturbation theory. The condition for $u_2 = 0$ to be stable is $4\nu < 3$ which generates bounds for the critical exponents ν and ν_k , namely,

$$\nu < \frac{1}{2} ; \quad \nu_k > \frac{6-d}{3} : \quad (58)$$

If the stability condition $4\nu < 3$ or equivalently, the second bound of Eq. (58), is violated at some dimension d , the fixed point structure of the theory changes fundamentally. Now $u_2 \neq 0$ is stable, and Eq. (45) gives us the (exact) relations

$$4\nu - 3 = 9 - \frac{1}{2} \epsilon > 0 ; \quad \nu_k = \frac{1}{2} + \quad (59)$$

instead of Eqs. (49). We lose one condition, and this leads to two independent critical exponents, as opposed to a single one. Following the same analysis as before, we arrive at the relations

$$\nu_k = \frac{6-d}{3} ; \quad \nu_k > 0 ; \quad 1-\nu = 2 : \quad (60)$$

The scaling behavior of the Green functions still follows Eq. (53), but ν_k can no longer be related to ν .

4. The roughness exponents

The roughness exponents of the surface are easily identified, once the scaling properties of the underlying field theory are known. For isotropic theories, they can be read off directly from the height-height correlation function,

$$G_{2,0}(\mathbf{r}-\mathbf{r}^0; t-t^0) = C(\mathbf{r}-\mathbf{r}^0; t-t^0) \langle h(\mathbf{r}; t) h(\mathbf{r}^0; t^0) \rangle$$

if its asymptotic scaling behavior of can be written in the form

$$C(\mathbf{r}; t) = \bar{r}^2 \bar{c}(\bar{t} = \bar{r}^z) \quad (61)$$

Here, α denotes the roughness exponent and z the dynamic exponent of the surface while c is a universal scaling function. Similarly, in Fourier space, the behavior of $C(r;t)$ translates into

$$C(q;t) = |q|^{-(d+2-\alpha)} e(t|q|^z) \quad (62)$$

with the same roughness exponent α . In our case, the situation is slightly more subtle [33], due to the presence of strong anisotropy [34]. First of all, surface fluctuations along the parallel and the transverse directions in real space need not be controlled by the same indices, leading us to define two exponents, α_\parallel and α_\perp , via

$$\begin{aligned} C(x_\parallel = 0; r_\perp; t) &= |r_\perp|^{2-\alpha_\perp} c_\perp(t|r_\perp|^z) \\ C(x_\parallel; r_\perp = 0; t) &= |x_\parallel|^{2-\alpha_\parallel} c_\parallel(t|x_\parallel|^{z=(1+\beta)}) \end{aligned} \quad (63)$$

A similar situation should be expected in Fourier space, prompting us to define two additional exponents, α_\parallel and α_\perp , via

$$\begin{aligned} C(0; q_\perp; t) &= |q_\perp|^{-(d+2-\alpha_\perp)} e_\perp(t|q_\perp|^z) \\ C(q_\parallel; 0; t) &= |q_\parallel|^{-(d+2-\alpha_\parallel)} e_\parallel(t|q_\parallel|^{z=(1+\beta)}) \end{aligned} \quad (64)$$

Of course, all of these expressions are only meaningful if the four scaling functions c_\parallel , c_\perp , e_\parallel and e_\perp approach finite and non-zero constants when their arguments vanish. Generically, the four roughness exponents take different numerical values; however, they can all be expressed in terms of the exponents α and β , according to the identities

$$\begin{aligned} \alpha_\parallel &= \frac{1}{2} [4 - (d + \beta)] & \alpha_\perp &= \frac{1}{2} [4 - (d + \beta)] - (1 + \beta) \\ \alpha_\parallel &= \frac{1}{2} [4 - d] & \alpha_\perp &= \frac{1}{2} [4 - \beta - (1 + \beta)] - \frac{d}{2} \end{aligned} \quad (65)$$

The key observation is that $\alpha_\parallel = \alpha_\perp = \alpha = \alpha_\parallel$ only if the anisotropy exponent vanishes.

In the following, we explicitly compute the roughness exponents for the two cases (i) and (iii). For case (ii), the renormalization group gives us no such information, since that would require the existence of an infrared stable fixed point. If, in fact, the presence of a first order transition line were to be confirmed eventually, the whole concept of scaling exponents would be inapplicable here.

Case (i) For this theory, characterized by positive β while α vanishes, we found that all exponents could be expressed in terms of $\beta = \frac{2}{3} + O(\epsilon^2)$. Writing all four roughness exponents in terms of this single index, we arrive at expressions which are exact to all orders in $\epsilon = 3 - d$:

$$\begin{aligned} \alpha_\parallel &= 1 - d/3; & \alpha_\perp &= \frac{1 - d/3}{3 - d/3}; \\ \alpha_\parallel &= (4 - d)/2; & \alpha_\perp &= \frac{4}{2(3 - d/3)} - \frac{d}{2}; \end{aligned} \quad (66)$$

The mean-field values are easily recovered by setting $\epsilon = 0$. The physically most interesting case corresponds to a surface grown on a two-dimensional substrate, i.e.,

$d = 2$ and $\epsilon = 1$. For this situation, one obtains $\gamma = 1/3$ and $\gamma_k = 1/9 + O(\epsilon^2)$ while $\gamma_k = 2/9 + O(\epsilon^2)$ and $\gamma_\perp = 4/3 + O(\epsilon^2)$. Remarkably, the exponent $\gamma = 1/3$ is actually exact, at least to all orders in perturbation theory.

Case (iii): At the multicritical point one has $\epsilon = 0$, $z = 4$, and a nontrivial γ . Hence, one obtains

$$\begin{aligned} \gamma &= [4 - (d + \epsilon)]/2 & \gamma_k &= \frac{4 - (d + \epsilon)}{2(1 + \epsilon)} \\ \gamma_\perp &= [4 - d]/2 & \gamma_k &= \frac{2}{(1 + \epsilon)} - \frac{d}{2} \end{aligned} \quad (67)$$

All of them are negative near the upper critical dimension $d_c = 6$. In order to access the physical ($d = 2$) situation, one has to set $\epsilon = 4$ here which gives a huge anisotropy exponent, $\gamma \approx 16.814$, if one naively uses the one-loop results. While roughness exponents can in principle be calculated, it does not appear meaningful to compare them to experimental data. Yet, we emphasize again that the exponents calculated here do not agree with [17].

5. Conclusions

To summarize, we have analyzed the effect of strong anisotropies on the universal behavior of a surface grown under ideal MBE-type conditions. The anisotropy is generated by an incident particle beam which is tilted away from the normal. This arrangement manifestly breaks rotational invariance in the substrate plane. As a consequence, the effective surface tension becomes anisotropic, being characterized by two parameters, γ_k and γ_\perp , as opposed to a single one in the isotropic case. If both are positive, the surface is described by the Edwards-Wilkinson model. However, as temperature or other growth parameters are varied, the two control parameters need not vanish simultaneously, leading to different dynamic and spatial instabilities and ordered structures. Clearly, there are three distinct scenarios: (i) $\gamma_k > 0$ while γ_\perp goes to zero, (ii) $\gamma_k \neq 0$ while γ_\perp remains positive, and (iii) both parameters vanish. Each of these three cases is described by its own characteristic field theory with distinct upper critical dimensions: $d_c = 3$, $7/2$, and 6 for cases (i), (ii), and (iii), respectively. To display scale-invariant behavior in the long-time, large-distance limit, a field theory must possess one, or more, infrared stable fixed points. Our one-loop analysis reveals that only cases (i) and (iii) have this property. In contrast, case (ii) may correspond to a line of first-order phase transition whose characteristics lie outside the scope of our RG techniques. For the two scale-invariant theories, we find two distinct, novel surface universality classes, and derive the associated scaling behavior of the height-height correlation function. An intriguing feature of both universality classes is the emergence of a strong anisotropy exponent, which reflects different scaling behavior in the parallel and transverse directions. As an immediate consequence, we need to introduce four different roughness exponents, to characterize surface fluctuations in real

and momentum space, observed along the parallel vs the transverse directions. While all four are related by exponent identities, care must nevertheless be exercised when analyzing experimental data.

We conclude with a few comments on the phase diagram. The first case clearly corresponds to a second order line, parameterized by κ . Assuming that the first order nature of the second case, parameterized by γ , can be confirmed, the third case $\kappa = \gamma = 0$ would turn out to be a critical endpoint. Since it requires the tuning of two parameters, it may be quite difficult to access in a typical experiment. In contrast, either the second or the first order lines should be more easily observable. From an RG perspective, even if the $\kappa \partial_k^2 h$ term is absent initially, it is immediately generated under RG transformations, leading to a non-zero critical value of κ ; this is not the case for the $\gamma r \partial_\gamma^2 h$ contribution. For this reason, we believe that the most physically relevant theory (beyond Edwards-Wilkinson behavior) is the one with $\kappa > 0$ and $\gamma = 0$. Our key results for this model are the roughness exponents for real-space surface scans. For a two-dimensional surface embedded in a three-dimensional space, we find $\gamma = 1/3$ for scans along the transverse direction, and $\kappa = 1/9 + O(\epsilon^2)$ for parallel scans. There appears to be some experimental evidence for these exponents [33] but more data are needed before this issue can be settled.

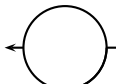
We thank U.C. Tauber, R.K.P. Zia, J. Krug, A. Hartmann, and E. Yewande for helpful discussions. This work is partially supported by the NSF through DMR-0308548 and DMR-0414122. GP acknowledges the Alexander von Humboldt foundation for their support.

Appendix

In the following, some technical details of the above calculations are presented. We prefer the time-momentum representation of the propagators and correlators, since it displays the causal structure of the Feynman diagrams most directly. In this representation, each $\Gamma_{1,1}$ - (or self energy) diagram has a single \tilde{h} -leg at the outgoing vertex with the largest time argument, and a single \tilde{h} -leg at the incoming vertex with the smallest time argument. To find the UV divergent $\Gamma = 0$ contribution, we just integrate over the time difference of these two vertices.

Appendix A. Case (i): $\gamma \neq 0$ and $\kappa \neq 0$

To characterize the theory fully, it suffices to calculate the vertex function $\Gamma_{1,1}$. The only one loop diagram which must be evaluated is

$$\Gamma_{1,1}(q; \epsilon) = G_0(q; \epsilon)^{-1} \left(\text{diagram} \right) + \dots \quad (\text{A } 1)$$


using the diagrammatic building blocks associated with Eqs. (11) and (12). This graph represents the one loop contribution to the self-energy. After integrating over the time

difference of the two vertices, it takes the form

$$\text{Diagram} = \int \frac{d^d p}{(2\pi)^d} \frac{[(q_\perp^2)^2 p_k^2 + 2q_\perp^2 (q_\parallel - p) p_k^2 + q_k^2 (p_\perp^2)^2]}{(p) [(p) + (q - p)]} \quad (\text{A } 2)$$

Several finite terms have been dropped, following a dimensional regularization and minimal subtraction scheme. The function (p) contains, up to a factor, the full momentum dependence of the inverse propagator

$$(p) = p_\perp^2 (p_\perp^2 + \gamma) + p_k^2 \kappa \quad (\text{A } 3)$$

Dimensional analysis immediately suggests that the terms in the bracket of Eq. (A 2) diverge logarithmically, except possibly the term $2q_\perp^2 (q_\parallel - p) p_k^2$, which is, at least naively, linearly divergent. The denominator in Eq. (A 2) is now expanded in small external momenta, and multiplied with the numerator, keeping only divergent contributions. After some straightforward algebra, we arrive at

$$(\text{A } 2) = \int \frac{1}{2} (q_\perp^2)^2 I(2;0;2) + \frac{1}{2} q_k^2 I(0;4;2) + \frac{2}{d-1} (q_\perp^2)^2 I(2;4;3) \quad (\text{A } 4)$$

The integrals $I(\dots)$ are defined as

$$I(\dots) = \int \frac{d^d p}{(2\pi)^d} \frac{p_k (p_\perp^2)^{-2}}{(p)} / \quad d+1+2+\dots \quad (\text{A } 5)$$

with the proportionality indicating the degree of divergence based on simple power counting in $d = d_c = 3$. Clearly, all integrals appearing in Eq. (A 4) are only logarithmically divergent; the (naive) linear divergence vanishes by symmetry. Using the effective coupling u introduced in Eq. (21), the integrals are

$$\int I(2;0;2) = \frac{u^2}{2''}; \quad \int I(0;4;2) = \frac{u^2}{2''} \kappa; \quad \int I(2;4;3) = \frac{u^2}{8''}; \quad (\text{A } 6)$$

and one finally arrives at Eq. (20).

Appendix B. Case (ii): $\kappa \neq 0$ and $\gamma \neq 0$

The diagrammatic representation of $\chi_{1,1}$, to one loop, is again given by Eq. (A 1). However, the relevant interaction vertex here is κ , so that the one loop integral reads

$$\int \frac{d^d p}{(2\pi)^d} p_k^2 (q_k - p_k)^2 \frac{1}{(p) [(p) + (q - p)]} \quad (\text{B } 1)$$

and the momentum dependence of the inverse bare propagator is controlled by

$$(p) = p_k^2 (\kappa p_k^2 + \gamma) + \gamma p_\perp^2 \quad (\text{B } 2)$$

As in the previous section, the integral (B 1) cannot be performed in closed form. Again, we expand the denominator of Eq. (B 1) in powers of q_k and q_\perp , noting that higher orders

become more and more convergent. Keeping only divergent terms, the singular part of $\Gamma_{1,1}$ takes the form

$$\Gamma_{1,1} = i! + \alpha_k^2 (k \alpha_k^2 + k) + \gamma \alpha_k^2 \int \frac{d^d p}{(2\pi)^d} \frac{p_k^4}{2(p)^2} \quad (B.3)$$

$$+ \int \frac{d^d p}{(2\pi)^d} \left(\frac{p_k^2}{2(p)^2} - \frac{7}{2} \frac{k p_k^6}{(p)^3} + \frac{4}{2} \frac{k^2 p_k^{10}}{(p)^4} + \dots \right) + O(k^{-4}) :$$

The leading singularity, i.e., the first integral above, is found to be quadratically divergent. It contributes to the renormalization of k and can therefore be controlled by an additive renormalization. We shift the critical parameter by an amount k_{rc} , defined through the vanishing of the parallel susceptibility, Eq. (15). Evaluating k to first order yields

$$k = k_c \int \frac{d^d p}{(2\pi)^d} \frac{p_k^4}{2(p)^2} + O(k^{-4}) : \quad (B.4)$$

The general renormalization scheme, Eq. (17), then allows us to determine

$$k_{rc} = k_c \int \frac{d^d p}{(2\pi)^d} \frac{p_k^4}{2(p)^2} + O(k^{-4}) : \quad (B.5)$$

$k=0$

in one loop. Reparameterizing $\Gamma_{1,1}$ in terms of the shifted k subsequently removes the quadratic divergence and leaves us with logarithmic divergences only. Hence, the vertex function reads, to first order,

$$\Gamma_{1,1} = i! + \alpha_k^2 (k \alpha_k^2 + k) + \gamma \alpha_k^2 + \alpha_k^2 \hat{\alpha}_k J(6;3)$$

$$+ \frac{1}{2} \alpha_k^4 J(2;2) - \frac{7}{2} k J(6;3) + 4 \alpha_k^2 J(10;4) + \dots$$

with the integrals $J(\cdot; \cdot)$ defined by

$$J(\cdot; \cdot) = \int \frac{d^d p}{(2\pi)^d} \frac{p_k}{(p)} / (2d-1) \quad (B.6)$$

Again, the proportionality indicates the degree of divergence based on $d = d_c = 7/2$. Using the effective coupling u introduced in Eq. (38), the integrals can be evaluated:

$$\alpha_k^2 J(2;0;2) = k \frac{4u^2}{3\pi} ; \quad \alpha_k^2 J(6;0;3) = \frac{u^2}{2\pi} ; \quad \alpha_k^2 J(10;0;4) = k^{-1} \frac{7u^2}{24\pi} ; \quad (B.7)$$

which finally results in Eq. (37).

Appendix C. Case (iii): $k \neq 0$ and $\gamma \neq 0$

The calculation of the selfenergy follows the same standard methods as above. However, the technical details become more involved, for two reasons. First, the full momentum dependence of the inverse propagator,

$$(p) = p_\gamma^2 (p_\gamma^2 + \gamma) + 2p_\gamma^2 p_k^2 + p_k^2 (k p_k^2 + k) \quad (C.1)$$

comes into play, with the two critical parameters, τ_c and k_c , serving as infrared cut-offs. Second, both nonlinearities, parametrized by k_c and τ_c , are now marginal at the upper critical dimension $d_c = 6$.

As before, we start with the diagrammatic representation, Eq. (A.1). Due to the presence of the full vertex, Eq. (12), the one-loop integral is given by

$$\int \frac{d^d p}{(2\pi)^d} \frac{V(fq; pg)}{(p) [(p) + (q - p)]}$$

where $V(fq; pg)$ summarizes the momenta contributed by the vertices:

$$\begin{aligned} V(fq; pg) &= \frac{1}{2} q_k^2 p_k^2 q_k p_k^2 \\ &+ \frac{1}{2} (q_k^2 p_k^2 + q_k^2 p_k^2 + q_k^2 p_k^2 + q_k^2 p_k^2) \\ &+ \frac{1}{2} (q_k^2 p_k^2 + q_k^2 p_k^2 + q_k^2 p_k^2 + q_k^2 p_k^2) \end{aligned}$$

As for case (ii), a shift of the critical parameter k_c absorbs a quadratic divergence in $\chi_{1,1}$. Demanding that the inverse (parallel) susceptibility, Eq. (15) vanishes at the true critical point, one finds in one loop order

$$\chi_{1,1}^{-1} = \int \frac{d^d p}{(2\pi)^d} \frac{p_k^4}{2(p)^2} - \int \frac{d^d p}{(2\pi)^d} \frac{(p_k^2)^2}{2(p)^2} \quad (C.2)$$

Again, we retain only logarithmic divergences in $\chi_{1,1}$ if we reparametrize it in terms of a shifted k_c ! $k_c \rightarrow k_{c,0}$. Expanding the denominator to $O(q^2)$ results in a sum of integrals of the form

$$I(\tau; k; \tau) = \int \frac{d^d p}{(2\pi)^d} \frac{p_k (p_k^2)^{-2}}{(p)} / \quad (C.3)$$

Formally, these look like Eq. (A.5), but it is essential to realize that (p) takes the more complicated form (C.1). To evaluate the $I(\tau; k; \tau)$, it is convenient to introduce a new integration variable, $x = q_k = j_1 j_2$ to replace q_k . This has the significant advantage that all τ -poles are already explicitly displayed, once the q_k -integration has been performed. The remaining integrals over x can be evaluated at $\tau = 0$ and are perfectly straightforward. They take the form

$$K_n(\tau) = \int_0^1 dx \frac{x^2}{(1 + 2wx^2 + x^4)} \quad (C.4)$$

with $(n; \tau) \in \{1; 0\}; \{2; 0\}; \{3; 0\}; \{4; 0\}; \{2; 1\}; \{3; 1\}; \{4; 1\}$. Clearly, these K 's lead to w -dependent coefficients for the different contributions to $\chi_{1,1}$. The result is summarized in Eq. (42) with the w -dependent functions

$$\begin{aligned} A_1 &= 2(1 + w); \\ B_1 &= 3; \quad B_2 = (5 + 2w); \quad B_3 = 3(7 + 2w(5 + 2w)); \\ C_1 &= (3 + w); \quad C_2 = 5 + 9w + 10w^2 + 4w^3; \\ D_1 &= \frac{1}{5}(7 + 5w); \quad D_2 = \frac{1}{5}(49 + 65w + 26w^2); \quad D_3 = \frac{1}{5}(10 + 2w); \end{aligned} \quad (C.5)$$

Tallying up all the contributions to $\chi_{1,1}$, and removing the divergences by renormalization, one arrives at the Z -factors listed in Eq. (43).

- [1] T. Halpin-Healey, Y.-C. Zhang, *Phys. Rep.* 254, 215 (1995)
- [2] J. Krug, *Adv. Phys.* 46, 139 (1997)
- [3] P. Meakin, *Phys. Rev. A* 38, 994 (1988)
- [4] P. Meakin and J. Krug, *Europhys. Lett.* 11, 7 (1990)
- [5] P. Meakin and J. Krug, *Phys. Rev. A* 46, 3390 (1992)
- [6] J. Krug and P. Meakin, *Phys. Rev. A* 40, 2064 (1989)
- [7] M. Kardar, G. Parisi, and Y. Zhang, *Phys. Rev. Lett.* 56, 889 (1986)
- [8] S. Bales, A.C. Redfeld, and A. Zangwill, *Phys. Rev. Lett.* 62, 776 (1989)
- [9] F. Ojeda, R. Cuerno, R. Salvarezza, and L. Vazquez, *Phys. Rev. Lett.* 84, 3125 (2000)
- [10] M.A. Mckeever, R. Cuerno, A.-L. Barabasi, *Nucl. Instr. and Meth. in Phys. Res. B* 197, 185 (2002)
- [11] D.E. Wolf, *Phys. Rev. Lett.* 67, 1783 (1991)
- [12] T. Hwa, *Phys. Rev. Lett.* 69, 1552 (1992)
- [13] U.C. Tauber and E. Frey, *Europhys. Lett.* 59, 655 (2002)
- [14] *Kinetics of Ordering and Growth at Surfaces*, edited by M. Lagally (Plenum, New York 1990)
- [15] S. DasSarma, *Comp. Mat. Sc.* 6, 149 (1996)
- [16] J. Krug, *Physica A* 313, 47 (2002)
- [17] M. Marsili, A. Maritan, F. Toigo, and J.R. Banavar, *Europhys. Lett.* 35, 171 (1996)
- [18] D.E. Wolf and J. Villain, *Europhys. Lett.* 13, 389 (1990); Lai, DasSarma, 1991Z.-W. Lai and S. DasSarma, *Phys. Rev. Lett.* 66, 2348 (1991)
- [19] J. Villain, *J. Phys. I (France)* 1, 19 (1991).
- [20] H.K. Janssen, *Phys. Rev. Lett.* 78, 1082 (1996)
- [21] H.J. Leamy, G.H. Gilmer, and A.G. Dicks, in *Current Topics in Materials Science*, Vol. 6, edited by E. Kaldis (North-Holland, Amsterdam, 1980); A.D. Mazor, J. Srolovitz, P.S. Hagan, and B.G. Bukiet, *Phys. Rev. Lett.* 60, 424 (1988); M. Marsili, A. Maritan, F. Toigo, and J.R. Banavar, *Rev. Mod. Phys.* 68, 963 (1996)
- [22] W.W. Mullins, *Solid surface morphologies governed by capillarity*. In: *Metal Surfaces: Structure, Energetics and Kinetics*, edited by N.A. Gjostein and W.D. Robertson (Metals Park, Ohio: American Society of Metals 1963)
- [23] R.L. Schwoebel and E.J. Shipsey, *J. Appl. Phys.* 37, 3682 (1966)
- [24] R.L. Schwoebel, *J. Appl. Phys.* 40, 614 (1969)
- [25] T. Sun, H. Guo, and M. Grant, *Phys. Rev.* 40, 6763 (1989)
- [26] S.F. Edwards and D.R. Wilkinson, *Proc. R. Soc. Lond. A* 381, 17
- [27] H.K. Janssen, *Z. Phys. B* 23, 377 (1976); R. Bausch, H.K. Janssen, and H. Wagner, *Z. Phys. B* 24, 113 (1976); H.K. Janssen, in *Dynamical Critical Phenomena and Related Topics (Lecture Notes in Physics, Vol. 104)*, edited by C.P. Enz, (Springer, Heidelberg, 1979)
- [28] C. DeDominicis, *J. Phys. (France) Colloq.* 37, C247 (1976); C. DeDominicis and L. Peliti, *Phys. Rev. B* 18, 353 (1978)
- [29] H.K. Janssen, in *From Phase Transitions to Chaos*, edited by G. Gyorgyi, I. Kondor, L. Sasvari, and T. Tel, (World Scientific, Singapore, 1992)
- [30] D.J. Amit, *Field Theory, the Renormalization Group and Critical Phenomena*, 2nd revised edition, (World Scientific, Singapore, 1989)
- [31] J. Zinn-Justin, *Quantum Field Theory and Critical Phenomena*, 3rd edition (Clarendon, Oxford, 1996)
- [32] F.J. Wegner, in *Phase Transitions and Critical Phenomena*, Vol. 6, eds. C. Domb and M.S. Green (Academic Press, New York, 1976)
- [33] B. Schmittmann, Gunnar Pruessner, and H.K. Janssen, to be submitted to *Physical Review B* (2006).
- [34] This is analogous to the scaling of driven diffusive systems and Lifshitz points. See, e.g., B. Schmittmann and R.K.P. Zia, in *Phase Transitions and Critical Phenomena*, Vol. 17, eds. C. Domb and J.L. Lebowitz (Academic Press, New York 1995).